Title: Numerical modelling of non-confined and confined masonry walls

Authors: P. Medeiros, G. Vasconcelos, P.B. Lourenço* and J. Gouveia

ISISE, Department of Civil Engineering, University of Minho, Guimarães, Portugal**;**
Corresponding author. Tel.: +351 253 510200; fax: +351 253 510217; E-mail address:
pbl@civil.uminho.pt

Abstract

This paper presents a discussion on the behaviour of non-confined and confined
masonry walls with different types of horizontal reinforcement when subjected to in-
plane horizontal loads, using advanced numerical simulations. An isotropic continuum
nonlinear finite element macromodel, based on a smeared crack total strain-stress
models with scarce parameter input is used to represent previously tested masonry
walls. The masonry units, the mortar and the bonding interfaces between the units and
mortar have been lumped in continuum elements. The input data is based on
experimental results or inverse fitting, with a clearly identification and justification. The
results are presented and compared against experimental data, with an emphasis on
force-displacement curves and failure modes.

Keywords:

Non-confined/Confined masonry; Horizontal reinforcement; Finite element nonlinear
analysis; Smeared cracking

1 INTRODUCTION

Due to its mechanical properties, durability and comfort masonry is an adequate choice as a structural material, which can be used in a wide range of typologies, namely arches, vaults or walls. Still, the use of masonry as a structural material became less and less common since the widespread of reinforced concrete after the end of the nineteenth century. In Portugal, particularly after the Second World War, the building sector was characterized by a rapid evolution in construction methods towards the use of reinforced concrete, which became the main structural system for new construction. Recent studies [1] estimate that reinforced concrete is used in about 90% of the new buildings in Portugal, while most European countries, e.g. Italy, Germany, the Netherlands or Denmark, still adopt masonry as the main competitive system for housing (30 to 50%). The European structural codes allow efficient design using different materials and the increasing interest of the scientific and technical community allow to believe that masonry will remain competitive and might increase competitiveness in countries that have lost this tradition.

Walls represent the main resisting structural element in masonry buildings ensuring resistance not only to vertical loading but also to wind or seismic loading, in earthquake prone areas. Recent earthquakes have shown that non-engineered unreinforced masonry systems, even if not so old, do not behave adequately for seismic loading, exhibiting brittle response and damage [2]. This behaviour is mainly attributed to the low strength of unreinforced masonry walls under tensile stresses induced by lateral loading, by insufficient robustness of the units and inadequate connection between floors and walls. The introduction of distributed reinforcement or confining elements improves significantly the seismic performance of masonry elements, leading to higher lateral

resistance and ductility ([3], [4], [5], [6]). Confined masonry, in which masonry walls are confined by vertical and horizontal reinforced concrete small elements (posts and lintels), has shown very satisfactory behaviour during moderate and strong earthquakes [7]. According to Tomažević and Klemenc [8] the confining elements prevent disintegration and improve ductility.

In the last years, externally funded research projects have been carried out at University of Minho, aiming at proposing different solutions for structural masonry walls, able to be used in low to medium rise residential buildings. The solution detailed here is based on lightweight concrete masonry walls with different typologies. Besides unreinforced masonry walls, to be used in areas with low seismic hazard, light horizontally reinforced masonry walls and confined masonry walls have been studied in detail.

The masonry research carried out in the last decades, both experimentally and numerically, has increased significantly the understanding of masonry as a composite material. Still, the knowledge and code drafting on structural masonry is far less consensual than reinforced concrete or steel. Even if it is possible to safely estimate the lateral resistance standard masonry walls under in-plane loading based on design codes, new solutions for masonry walls require their mechanical validation through experimental testing. In the case of confined masonry and lightly bed joint reinforced masonry, the available knowledge is moderate. Testing is expensive and takes time but is the best way to provide the strength, the capacity to dissipate energy and the failure modes of non-conventional solutions. Still, less expensive and less time consuming alternatives for testing need to be used, if not to replace them, at least, to complement them.

This article aims at demonstrating that reasonable results for masonry capacity can be obtained using low parameter demanding, commercially available, constitutive models. For this purpose, a series of lightweight concrete masonry walls tested under in-plane cyclic loads are considered. The wall configurations tested range from unreinforced-non-confined up to horizontally reinforced-confined masonry. An overview of the experimental results is given first, with details and comparison between the distinct typologies. Finally, the quality of the numerical results is assessed and the shortcomings of using standard inelastic models are presented.

2 EXPERIMENTAL PROGRAM

The development of a structural masonry solution based on lightweight concrete blocks existing in the Portuguese market motivated an experimental campaign, co-sponsored by the block producer. The main goal was to define adequate a solution to be used in low to medium rise residential buildings (typically up to 4 stories), in regions of low to high seismicity in Portugal. Three different possibilities where conceived, based on masonry systems mentioned in Eurocode 6 [9]: 1) unreinforced; 2) reinforced and; 3) confined. The experimental program included tests to quantify the mechanical properties of units and mortar, wallets and shear walls, allowing to obtain: 1) the Young's modulus and compressive strength of masonry units and wallets, perpendicular to the bed joint; 2) the compressive strength of concrete and; 3) strength and ductility parameters of shear walls subjected to horizontal in-plane cyclic loads. The shear walks are subsequently used for comparison with numerical modelling and, therefore, are briefly addressed in the next sections.

2.1 Wall configurations and mechanical properties

As stated above, the in-plane cyclic tests aimed at the assessment of the strength and ductility properties of three distinct masonry wall systems (unreinforced, horizontally reinforced and confined). According to Eurocode 8 [10], masonry walls should have filled vertical joints when located in seismic regions. Still, this is complex for thick masonry blocks and reduces productivity. Therefore, it is worth to discuss the relevance of filling vertical joints, when bed joint reinforcement or confining elements exist. In this context, six wall configurations were built, with a total of 16 walls. Table 1 briefly details the several specimens tested.

Due to limitations in the laboratory, and in order to obtain representative masonry wall panels, it was decided to use half scale masonry units resulting from the cutting of real units to nominal dimensions of 200x143x100mm^3 (**Fig. 1**). These units only have half the height of a full size unit, allowing a modularity in height of 100 mm. The tested masonry wall panels were 1.0m height by 1.0m length (Fig. 2 a), resulting in a height to length ratio of 1.0. The normalized compressive strength of the unit is 5.7N/mm^2. The mortar adopted for the wall construction was pre-mixed, with 10 N/mm^2 compressive strength. It was decided to use this commercial mortar in order to comply with easier quality control of the construction. The class selected (M10) is the one normally used in Portugal. The wallets tested under compression perpendicular to the bead joint lead to an average strength of 2.8 N/mm^2. The concrete elements of the confining system were built using a self-compacting concrete with a compressive strength, f_{cm}, of 31.5N/mm^2. The adopted cross sections are 143x75mm^2 (vertical elements) and 143x80mm^2 (horizontal elements). The reinforcement consists of 4ϕ6mm steel bars (f_{yk}=400N/mm^2) with 4mm stirrups spaced at 75mm (f_{yk}=400N/mm^2). Bed joint reinforcement for

masonry is a truss type reinforcement with longitudinal bars of 5 mm diameter (f_{yk}=550N/mm^2). The configuration of the reinforcements of the confining elements is shown in Fig. 2 b. In the confined walls with a connection between the masonry wall and the confining elements (W2.6), the horizontal reinforcement is anchored to the vertical reinforcements of the confining columns.

2.2 In-plane experimental setup

The shear walls were tested using the layout shown in Fig. 3. The base was fixed to a rigid concrete floor in order to preclude any horizontal and vertical movement. The top of the wall is allowed to rotate, even if an eccentric horizontal load is applied at mid height. The eccentricity of this load aimed at preventing the predominance of flexural failure modes, detected in preliminary tests. The connection between the vertical and horizontal steel elements by which the horizontal load is applied was ensured through welding. The horizontal load is applied by means of a servo controlled hydraulic actuator with a double hinged connection to the reaction wall and to the vertical steel column. The pre-compression load was applied by using a vertical actuator with a maximum capacity of 250kN, being its reaction transferred to the strong floor by means of flexible vertical steel cables. The tests were carried out with constant vertical stress of about 0.9N/mm^2 corresponding to about 30% of the compressive strength of masonry. A stiff beam was used for the distribution of the vertical load and a set of steel rollers was also placed on the top, in order to allow relative displacements between the wall and the vertical actuator. The tests were carried out under displacement control, following the displacement history shown in Fig. 3.

2.3 Brief overview of the results from in-plane cyclic tests

In terms of crack patterns it was observed that in walls without bed joint reinforcement (W2.1, W2.2 and W2.4), horizontal flexural cracking at the heel of the

walls prevailed for low levels of horizontal displacement. With increasing lateral displacements, diagonal cracking suddenly developed, with a localized crack well defined, see Fig. 4. The diagonal crack in the specimen with vertical joints filled (W2.2) goes through units and mortar without a preferential path, a behaviour consistent with a good connection between the two materials that indicates a reasonably homogenous material.

In non-confined masonry specimens, W2.1, W2.2 and W2.3, the peak strength is reached before the appearance of a diagonal crack. Crushing in the toe occurs for larger displacements.

In the confined masonry walls, W2.4, W2.5 and W2.6, a shear crack is detected in the concrete node between post and lintel, which leads to failure of the wall. It is clear that when reinforcement is placed at bed joint, diagonal cracking is considerable more distributed, and with smaller crack width. In this case, a rather ductile behaviour was found, with low strength and stiffness degradation. The influence of bed joint reinforcement is particularly relevant in case of confined masonry walls, see Fig. 4. The enhancement of the lateral performance of confined masonry walls with anchored bed joint reinforcements is revealed by the very well distributed cracking in the walls, with small crack width and higher lateral resistance.

The influence of the confining elements is well observed through the force-displacement diagrams shown in Fig. 5. There is an improvement of the lateral behaviour in terms of dissipation of energy and deformation capacity (lateral drift increases from 0.20% to 0.26%). The behaviour of unreinforced masonry walls is practically linear until the maximum lateral resistance is reached, which reveals a

somewhat fragile behaviour, due to lack of robustness of the units. On the contrary, confined (unreinforced) masonry walls exhibit considerable strength and stiffness degradation after peak load, resulting in a more ductile response. In terms of lateral resistance an increase of 17% was observed in confined (unreinforced) masonry wall when compared to the unreinforced masonry walls. This result is in agreement with Tena-Colunga et al. [7] and Tomažević and Klemenc [8]. The increase on the lateral strength due to the addition of horizontal reinforcement in non-confined masonry, in comparison to non-confined unreinforced masonry, is about 10%, while the lateral drift increases from 0.20% to 0.41%. In confined masonry, when bed joint reinforcement is considered, an increase on the lateral resistance of approximately 20% and 28% was observed if the horizontal reinforcement is connected or not connected to the posts, respectively. The increase on the lateral drift from confined (unreinforced) masonry walls to confined bed joint reinforced masonry walls is about 0.19% (increase from 0.26% to 0.45%). It should be mentioned that the lateral drifts obtained for the confined masonry walls are, on average, in agreement with the ones pointed out by Ruiz-Garcia and Negrete [11], whom compiled the experimental results of several authors.

Finally, it should be mentioned that no significant differences were detected in the force-displacement diagrams of non-confined unreinforced masonry walls with filled and unfilled vertical joints. In terms of lateral strength, an increase of 10% was obtained in specimens with filled vertical joints. Similar behaviour has been found for brick masonry walls [12]. However, from diagonal compression tests carried out on square concrete block masonry wallets, it appears that filling of vertical joints can increase the shear and the tensile strength of masonry [13]. More details on the seismic performance of the masonry walls can be found in Gouveia and Lourenço [14].

3 NUMERICAL MODELLING

The understanding of the behaviour of masonry walls under in-plane loading can be significantly improved by numerical modelling. Modelling can be considered as auxiliary to experimental analysis, allowing the assessment of masonry systems behaviour when subjected to a wide range of conditions without the need of intensive experimental work.

Different approaches have been used to model masonry walls through the finite element method. The pioneer work of Lourenço [15] on the numerical strategies for modelling of masonry structures makes a distinction between detailed micro, simplified micro and macro numerical models. Detailed micro models consider masonry units, mortar and the unit-mortar interface as individual elements with distinct properties. Simplified micro models consider the mechanical characteristics of masonry units and mortar lumped in the same element and the unit-mortar interface as a distinct element with different properties. Macro models consider the masonry material as a continuum (the distinct material components of masonry are lumped in a homogeneous material), either with isotropic or anisotropic mechanical properties. When choosing the modelling approach for a given structure, the level of detail, the available time and quality of results should be balanced. Micro modelling is generally used when nonlinear features of the unit-mortar interfaces are important and when distinct failure patterns are to be captured. This approach has been used e.g. by Haach [5] for the numerical modelling of reinforced concrete block masonry under in-plane loading and of concrete block masonry beams under flexure and shear. The strong time demand for the analysis and the need of detailed information about the mechanical properties required in the micro-

modelling led to the preference for macro analysis in the present work. Macro models are usually adopted in engineering applications, e.g. [16].

3.1 Geometry, mesh, boundary and loading conditions

The numerical model proposed is a plane stress macro model. The geometry of the walls considered is similar to the one used in the experimental tests (1.0 x 1.0 m^2). A regular mesh with the discretization indicated in Fig. 6 was used. Three different types of finite elements were used to build the numerical models: 1) eight node continuum plane stress element with a 3x3 Gauss integration points to simulate masonry, concrete and steel beams; 2) six node interface elements with 3 Lobatto integration point to simulate the welded joint between the vertical and horizontal steel beams and; 3) bonded embedded reinforcement elements to simulate the reinforcement (in masonry, if applicable) and in the reinforced concrete confining elements (in confined masonry, if applicable). Even if other hypotheses have been considered, e.g. [17], the connection between masonry and concrete in confined walls was considered monolithic in the present work, as all tests carried out exhibited no separation. Note that the self-compacting concrete cast against the porous units lead to an excellent bonding interface between the two materials.

In terms of boundary conditions, the bottom of the walls was assumed as fully constrained, while the steel beams on top are rigidly connected to the masonry and concrete confining elements. The existence of a welded connection between the horizontal and vertical steel beams has been modelled by using an interface element that simulates the elastic connection between them.

Two types of loads representing the vertical compression and the envelope of the horizontal cyclic force have been applied. The vertical compression was applied

uniformly to the top of the steel beams and the horizontal load was considered as monotonic and was simulated by an explicit displacement applied with an eccentricity similar to the experimental one. The self-weight of masonry has been disregarded since its value is negligible, when compared to the vertical compression force. In the analysis the vertical compression was first applied, after which the horizontal displacement was gradually increased.

3.2 Material model used in numerical simulations

Five different materials are considered, if applicable to the respective wall: 1) steel beams; 2) welded interface; 3) reinforcement; 4) masonry and; 5) concrete. The steel beams and the interface that represents the weld are considered to behave linear elastically, as no damage was observed in the steel parts. The rest of the materials are considered with full nonlinear properties.

Masonry and concrete are considered to follow the same material model despite their different behaviours. An isotropic smeared crack model, with a fixed crack orientation and constant shear degradation has been chosen to represent both materials in the nonlinear stage. The model directly relates the principal stress with principal strain values computed for each load step in the element. The relation is made based on constitutive laws that describe the behaviour of the material in tension, compression and shear, before and after the appearance of cracks.

This model was selected to describe masonry mainly because of the limited data required. Masonry is anisotropic and it would be more adequate to use an anisotropic model, either continuum based as in [18] or mathematically homogenized as in [19] and

in [20]. Still, there is insufficient experimental information available and it is complex to test the masonry developed in the direction parallel to the bed joints. It is noted that, due to size of the lightweight aggregates, the units are only moderately perforated (about 30%) and the ratio of effective area in both directions is comparable. This means that the expected degree of anisotropy is low. Finally, it is noted that, particularly in the case of filled vertical joints, the cracks obtained in the shear wall tests cross the units and joints, further demonstrating a relatively homogeneous behaviour.

The Young's modulus in the direction perpendicular to the bed joint was available from tests but it was found that this value would lead to a very stiff response, as also obtained by other authors. The Young modulus adopted in the numerical model was, therefore, fitted to the experimental elastic stiffness observed in the in-plane tests, both for the unreinforced and non-confined specimen.

Additional information on the fracture properties of masonry and concrete is required, namely the tensile strength (f_t), compressive strength (f_c), tensile fracture energy (G_f), compressive fracture energy (G_c) and the shear retention factor (β). The compressive strength of masonry parallel to the bed joints (2.8 N/mm^2) was known from tests. The tensile strength of masonry has been determined indirectly, based on the relation proposed by Tassios [21], and taking into account that unreinforced masonry fails in shear by (eq. (1)):

$$H = A_w \left(\frac{f_t}{b} \sqrt{\frac{\sigma_0}{f_t} + 1} \right) \qquad \text{eq. (1)}$$

where H is the shear strength of unreinforced masonry obtained in experimental testing, A_w is the horizontal cross section of the wall, and f_t is the tensile strength of masonry

associated to the diagonal crack opening, σ_0 is the average normal stress, calculated as the ratio between the compressive load and the cross section of the wall, and b is the shear stress distribution parameter accounting for the geometry of the wall (1.5).

The shear retention factor is considered equal to 0.1, which is prevents excessive rotation of the principal stresses. The value adopted for the tensile fracture energy, G_f, follows the values proposed by Lourenço [15] and for the compression fracture energy, G_c, follows the recommendations given by Lourenço [22], see eq. (2), which is valid for compressive values below 12N/mm^2:

$$G_c = d_u \times f_k \qquad \text{eq. (2)}$$

where G_c is the compression fracture energy, d_u is the ductility factor, measured as the ratio between the fracture energy and the strength (tensile or compressive), and f_k is the characteristic compressive strength of masonry. A value of 1.6mm for the ductility factor has been used in this work, according to the value proposed in [22]. It is noted that the uniaxial tests aiming at characterizing the fragility of masonry were unsuccessful, indicating a rather brittle behaviour. It is known that there is limited information on the compressive fracture energy of masonry and that this information depends e.g. on the experimental set-up and boundary conditions. The values proposed, according to the authors' experience, provide reasonable results. This is confirmed by the results obtained in the numerical analysis, even when toe crushing of the walls is present.

For concrete, a value of the compressive strength of 31.5 N/mm^2 was obtained from experimental tests. The fracture energy parameters of reinforced concrete were determined based on the expressions presented in CEB-FIB [23], considering an

aggregate size of 8mm. Reinforcement steel has been considered to have an elastic-perfectly plastic behaviour with a yield strength f_{sy} of 550N/mm^2 for truss type masonry reinforcement and of 400 N/mm^2 for the reinforcement of the concrete confining elements.

The mechanical properties used for masonry, concrete and steel are summarized in Table 2. The Young's modulus of concrete and steel are based on CEB-FIP [23] recommendations. The uniaxial constitutive laws used for masonry are shown in Fig. 7. For concrete, similar laws are adopted, with the applicable strength and ductility. The quasi-brittle behaviour of these materials in tension is given by a diagram composed of a linear branch until the peak load and an exponential curve after peak. The compressive behaviour has been described by a composed diagram with a linear branch until one third of the peak load and a parabolic function starting from this point, until complete failure. Shear stiffness degradation is considered by a constant shear stiffness degradation. A thorough explanation about the material behaviour functions can be found in [24] and [25].

Finally, the normal and shear stiffness, k_n and k_s, considered for the interface elements representing the connection between the steel profiles for transmitting the horizontal loading was 25N/mm^3 and 10e+07N/mm^3, respectively. This means that no sliding is allowed, whereas the normal stiffness was calibrated from the experimental results.

3.3 Comparison between experimental and numerical models

In this section the comparison between the experimental and numerical results is performed. The analysis is based on the experimental force-displacement monotonic envelope and crack patterns, both for non-confined and confined masonry panels.

3.3.1 Non-confined and confined masonry walls

The comparison between the experimental and numerical results concerning the non-confined unreinforced and lightly bed joint reinforced walls is presented in Fig. 8. It is observed that the proposed numerical model is capable of detecting the major features of the experimental behaviour of these walls. Crack patterns and force-displacement diagrams are well reproduced. Note that only one diagonal crack is detected by the numerical simulation as only the monotonic load was considered in the model. As in the experimental tests, also in the numerical models, flexural horizontal cracks develop at early stages of lateral displacement, which are responsible for the beginning of the nonlinear behaviour. In unreinforced masonry walls, the peak load is limited by the development of a diagonal crack, after which a significant stiffness loss occurs. A good agreement between the numerical and experimental peak load was achieved for non-confined walls, being the average difference of the three walls about 6%. The influence of the filling of the vertical joints (wall W2.2) is well captured in terms of peak load and also on the increased brittleness of the post peak stage, as identified in the experimental tests. The effect of the horizontal reinforcement (wall W2.3) is also well captured, which provides a more distributed cracking and a smaller width of the localized diagonal crack. As in the tests, a more ductile behaviour is also obtained in this numerical analysis, with a longer tail of the post-peak branch. Still, the horizontal reinforcement did not have a visible contribution for the lateral peak load, which was also observed in the experimental response.

For confined masonry walls, the numerical models lead still to acceptable results for the stiffness in the pre- and post-peak stages, even if with larger deviation than before, see Fig. 9. Experimental and numerical peak loads are, on average, in good agreement

(8%), although obtained at somewhat different displacement levels. The crack pattern follows the sequence identified in the experimental tests for all the specimens. The first significant reduction in the stiffness occurs when a diagonal crack develops. The peak load is reached with the yielding, due to flexure, of the reinforcement of the post in the opposite side to the point of application of the load and at bottom corner of the walls. The more brittle behaviour of walls W2.4 and W2.5 in the experimental tests is associated to the development of shear cracks, which cannot be well described by the coarse numerical models adopted, and justifies the considerably more ductile behaviour found. As found in the non-confined masonry walls, also in the confined horizontally reinforced masonry walls (W2.5 and W2.6) a more distributed and smaller crack width is recorded. The different anchorage types between the masonry walls and the confining elements provide different ductility, even if numerically this is largely overestimated. The difference found can be possibly attributed to the perfect bond assumed for the reinforcement.

4 CONCLUSIONS

This paper deals with the experimental and numerical validation of a masonry wall system based on lightweight concrete masonry units, to be used in low to medium rise residential buildings in seismic areas. A general overview of the main experimental results of in-plane cyclic tests, using non-confined and confined masonry walls, was provided and a detailed description of its numerical modelling was also given. The input parameters for the material models have been determined from experimental tests and from guidelines available in the literature.

From the experimental analysis it was concluded that: (a) in non-confined masonry specimens the peak strength is attained before the appearance of a diagonal crack; (b) the diagonal crack in the specimen with filled vertical joints goes through units and mortar, without a preferential path, exhibiting a more fragile behaviour than the unreinforced masonry with unfilled vertical joints; (c) confined (unreinforced) masonry walls exhibit clearly an enhanced lateral behaviour with much higher dissipation of energy and deformation capacity, and with a moderate increase on the lateral resistance; (d) the addition of horizontal reinforcement leads to a more disperse and lower crack width, as well as to a more ductile behaviour both in confined and non-confined masonry walls; (e) the anchorage of horizontal reinforcement inside the tie columns leads to higher strength and ductility of the wall.

Despite the level of simplification of the proposed isotropic macro-model, a reasonable good agreement between experimental and numerical results for non-confined masonry walls was achieved, namely with respect to crack patterns and monotonic force-displacement envelopes. In the case of confined masonry the results for pre- and post-peak stiffness are less accurate, although the crack pattern sequence and the peak strength exhibit a good agreement. The interface between concrete and masonry and the shear stiffness degradation law considered may be responsible for the fair agreement and their influence should be investigated. In both cases, the stiffness, peak load and the more distributed crack patterns in the presence of bed joint truss type reinforcement are reasonably predicted.

5 REFERENCES

[1] Lourenço PB. Current experimental and numerical issues in masonry research. Proc 6th National Conference on Seismology and Seismic Engineering. Guimarães 2004. p. 119-36. Available from www.civil.uminho.pt/masonry.

[2] Klingner R. Behavior of masonry in the Northridge (US) and Tecomán–Colima (Mexico) earthquakes: Lessons learned, and changes in US design provisions. Construction and Building Materials. 2006; 20(4):209-19.

[3] Shing PB, Noland JL, Klamerus E, Spaeh H. Inelastic behavior of concrete masonry shear walls. Journal of Structural Engineering. 1989;115(9):2204-25.

[4] Shing PB, Schuller M, Hoskere VS. In-plane Resistance of reinforced masonry shear ealls. Journal of Structural Engineering. 1990;116(3):619-40.

[5] Haach VG. Development of a design method for reinforced masonry subjected to in-plane loading based on experimental and numerical analysis [PhDThesis]. Guimarães: Universidade do Minho; 2009. Available from www.civil.uminho.pt/masonry.

[6] Tomaževič M. Earthquake-resistant design of masonry buildings. Innovations in structures and construction. London: Imperial College Press; 1999.

[7] Tena-Colunga A, Juárez-Ángeles A, Salinas-Vallejo VH. Cyclic behavior of combined and confined masonry walls. Engineering Structures. 2009;31(1):240-59.

[8] Tomaževič M, Klemenc I. Seismic behaviour of confined masonry walls. Earthquake Engineering & Structural Dynamics. 1997;26(10):1059-71.

[9] CEN. Eurocode 6, EN 1996-1-1. Design of masonry structures - Part 1: General rules for reinforced and unreinforced masonry structures. Brussels: CEN; 2005.

[10] CEN. Eurocódigo 8, EN 1998-1: Design of structures for earthquake resistance - Part 1: General rules, seismic actions and rules for buildings. Brussels: CEN; 2009.

[11] Ruiz-Garcia J, Negrete M. Drift-based fragility assessment of confined masonry walls in seismic zones. Engineering Structures. 2009;31(1):170-81.

[12] Lourenço PB, Vasconcelos G, Medeiros P, Gouveia J. Vertically perforated clay brick masonry for loadbearing and non-loadbearing masonry walls. Construction and Building Materials. 2010; 24(11): 2317-30.

[13] V.G. Haach, Vasconcelos G, Lourenço PB. Influence of the geometry of units and of the filling of vertical joints in the compressive and tensile strength of masonry. Materials Science Forum 2010;Advanced Materials Forum V:1321-8.

[14] Gouveia JP, Lourenço PB. Masonry shear walls subjected to cyclic loading: influence of confinement and horizontal reinforcement. 10th North American Masonry Conference. St Louis, Missouri, USA2007. p. 838-48.

[15] Lourenço PB. Computational Strategies for masonry structures [PhD Thesis]. Delft: Delft; 1996. Available from www.civil.uminho.pt/masonry.

[16] Lourenço PB, Orduña A. Seismic Analysis and Strengthening of a 17th Century Church in Azores. 9th North American Masonry Conf. Clemson, USA2003. p. 932-41.

[17] Khashaiar P, Sassan E. Development of capacity curves for confined masonry walls. The Masonry Society Journal. 2009;27(1):21-34.

[18] Lourenço, PB, Rots, JG, Blaauwendraad, J, Continuum model for masonry: Parameter estimation and validation. Journal of Structural Engineering, ASCE. 1998;124(6):642-52.

[19] Zucchini, A., Lourenço, PB. Validation of a micro-mechanical homogenisation model: Application to shear walls. International Journal of Solids and Structures. 2009;46(3-4):871-86.

[20] Milani, G., Lourenço, PB, Tralli, A. Homogenised limit analysis of masonry walls. Part I: Failure surfaces. Computers & Structures. 2006;84(3-4):166-180.

[21] Tassios TP. Meccanica delle murature.Napoli: Liguori Editore;1988.

[22] Lourenço PB. Recent advances in masonry structures: Micromodelling and homogenisation. In: Galvanetto U, Aliabadi MHF, editors. London: Imperial College Press; 2009. p. 251-94.

[23] CEB-FIP. CEB-FIP Model Code 1990. London: Thomas Telford Services Ltd.; 1993.

[24] 90-FMA RTC. Fracture mechanics of concrete structures : from theory to applications : report / Technical Committee 90-FMA Fracture Mechanics to Concrete-Applications, RILEM ; ed. L. Elfgren. In: Hall Ca, editor. London1989.

[25] TNO D. DIANA – Finite Element Analysis - User's Manual – Material Library – Release 8.1. Delft, Netherlands: TNO Building and Construction Research; 2002.

Table 1. Type and designation of specimens tested.

Table 2. Input material parameters for the numerical model.

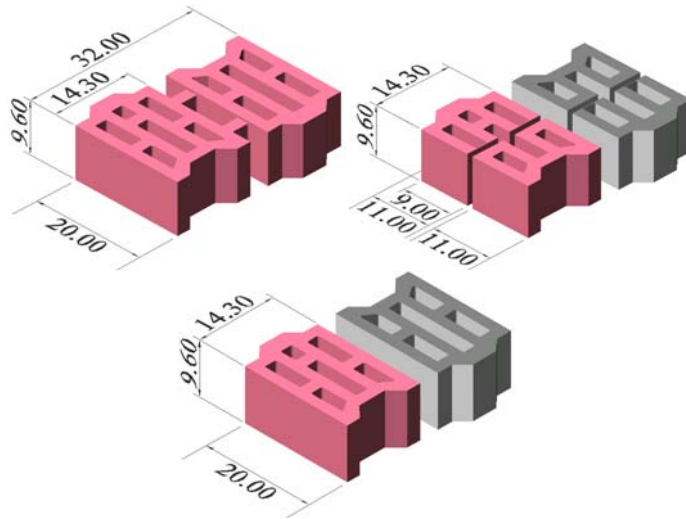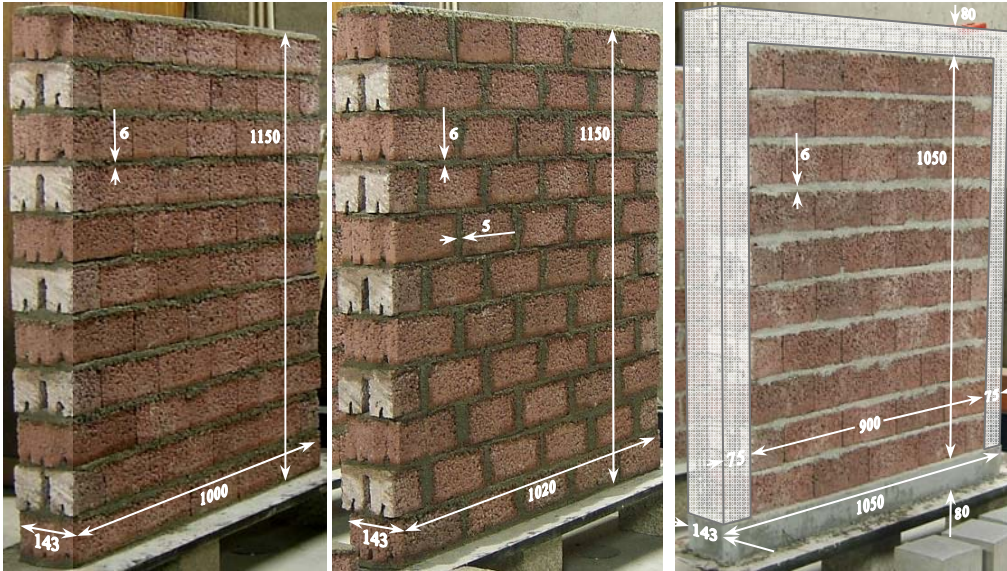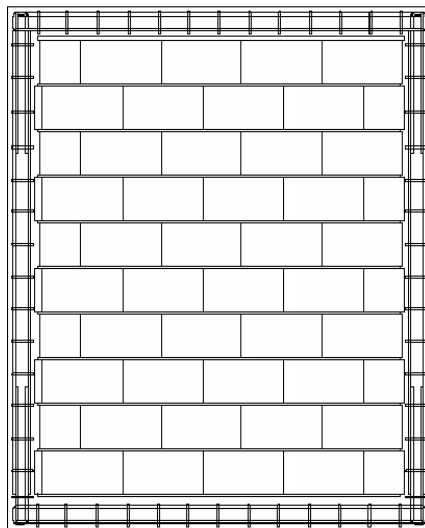**Fig. 1** Geometry and shape of the lightweight concrete masonry units

Fig. 2. Geometry of non-confined and confined lightweight masonry walls; (a) masonry specimens (dimensions in mm); (b) configuration of reinforcement for the confining elements.
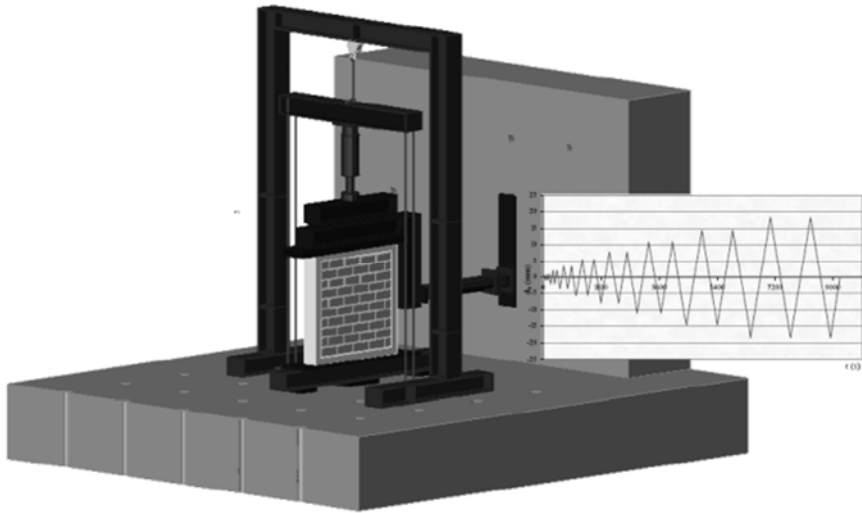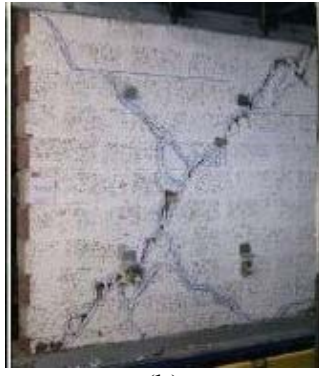
Fig. 3. Details from experimental tests: test setup and loading diagram

**Fig. 4.** Failure patterns; (a) wall W2.1; (b) wall W2.2; (c) wall W2.3; (d) wall W2.4; (e) wall W2.5; (f) wall W2.6.

Fig. 5. Typical force-displacement diagrams; (a) non-confined (unreinforced) masonry walls; (b) confined (unreinforced) masonry wall; (c) confined lightly bed joint reinforced masonry walls.

Fig. 6. Geometry and mesh details of finite element models for (a) non-confined and (b) confined masonry.

Fig. 7. Functions describing the behaviour of masonry in: a) tension and compression; b) and shear degradation.

Fig. 8. Comparison between the experimental and numerical models in terms of crack pattern (at final displacement) and force-displacement diagrams for non-confined walls; (a) non-confined and unreinforced masonry wall with unfilled vertical joints (W2.1); (b) non-confined and unreinforced masonry wall with filled vertical joints

(W2.2); (c) non-confined and horizontally reinforced masonry wall without vertical joints unfilled (W2.3).

Fig. 9. Comparison between the experimental and numerical models in terms of crack pattern (at maximum displacement) and force-displacement diagrams for confined walls a) unreinforced wall with vertical joints unfilled (W2.4); b) horizontally reinforced masonry with reinforcement anchored in the masonry, and with vertical joints unfilled (W2.5); c) horizontally reinforced masonry with reinforcement anchored in the concrete tie-columns, and with vertical joints unfilled (W2.6).

Fig. 1. Geometry and shape of the lightweight concrete masonry units (dimensions in cm).

(a)

(b)

Fig. 2. Geometry of non-confined and confined lightweight masonry walls;
(a) masonry specimens (dimensions in mm); (b) configuration of reinforcement for the
confining elements.

Fig. 3. Details from experimental tests: test setup and loading diagram.

Fig. 4. Failure patterns; (a) wall W2.1; (b) wall W2.2; (c) wall W2.3; (d) wall W2.4; (e) wall W2.5; (f) wall W2.6.
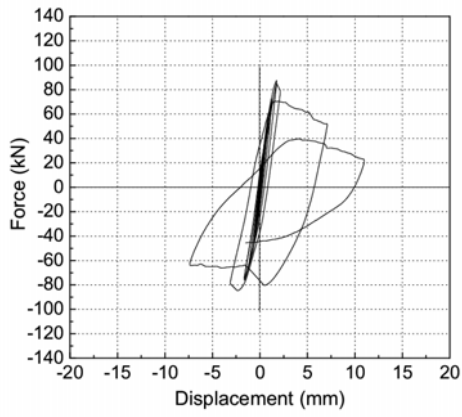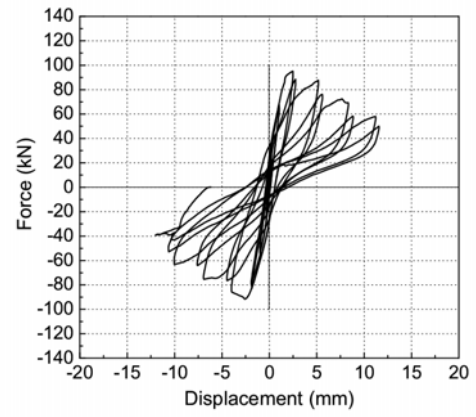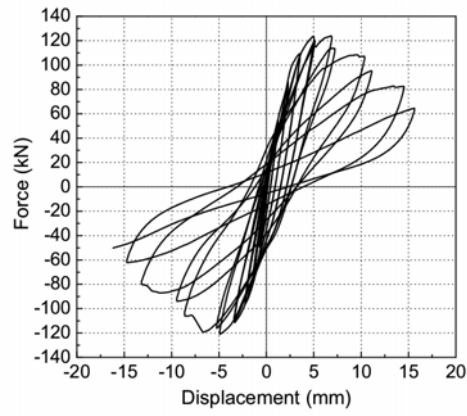
Fig. 5. Typical force-displacement diagrams; (a) non-confined (unreinforced) masonry walls; (b) confined (unreinforced) masonry wall; (c) confined lightly bed joint reinforced masonry walls.
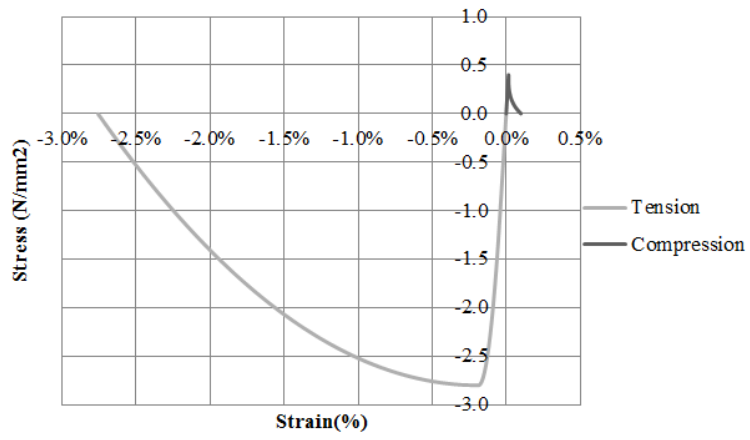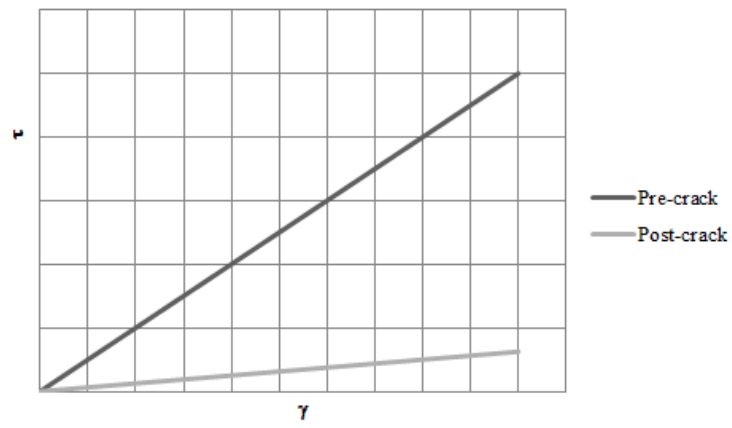
Fig. 6. Geometry and mesh details of finite element models for (a) non-confined and (b) confined masonry.

a)

b)

Fig. 7. Functions describing the behaviour of masonry in: a) tension and compression; b) and shear degradation.
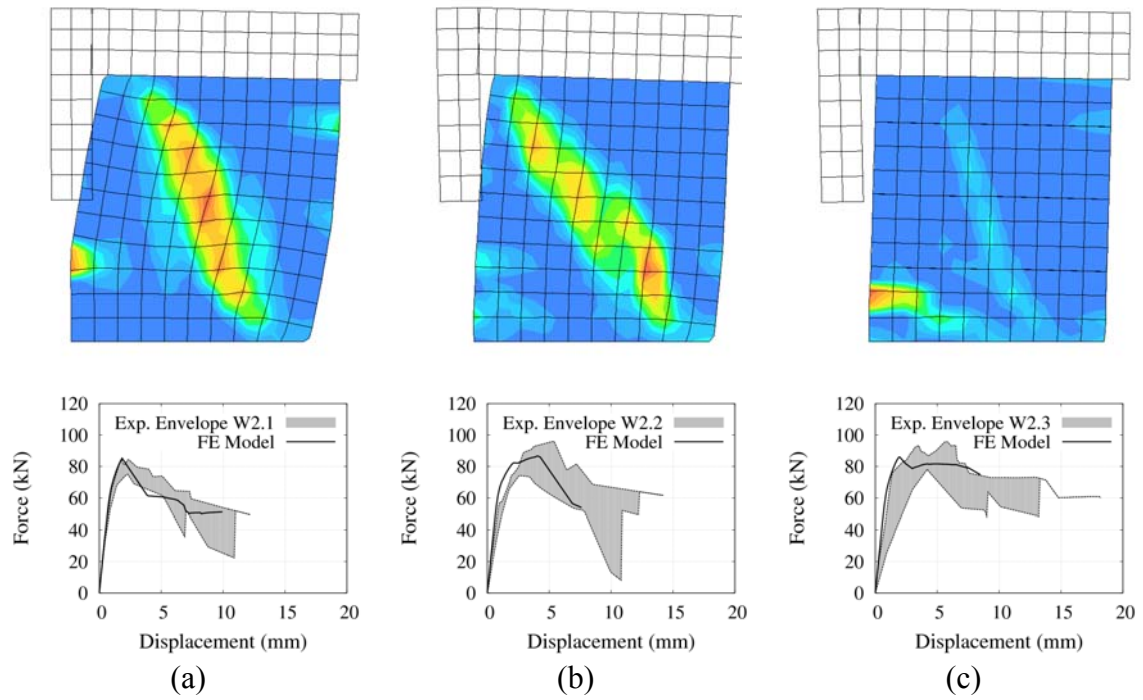
Fig. 8. Comparison between the experimental and numerical models in terms of crack pattern (at final displacement) and force-displacement diagrams for non-confined walls; (a) non-confined and unreinforced masonry wall with unfilled vertical joints (W2.1); (b) non-confined and unreinforced masonry wall with filled vertical joints (W2.2); (c) non-confined and horizontally reinforced masonry wall without vertical joints unfilled (W2.3).
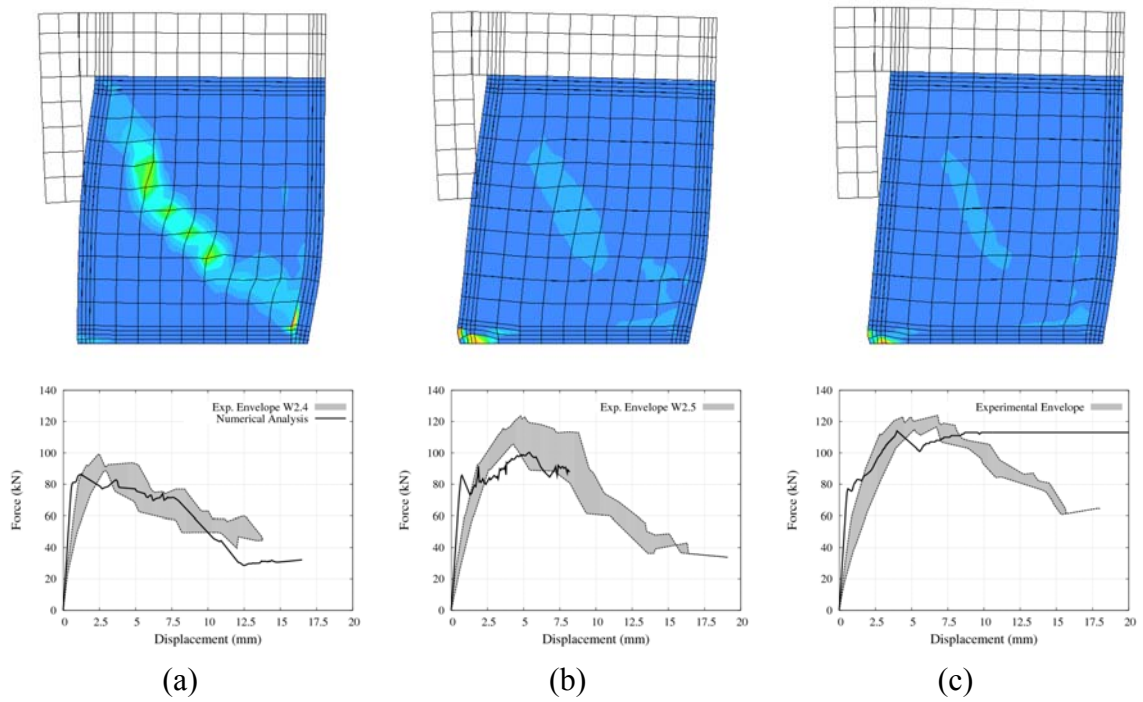
Fig. 9. Comparison between the experimental and numerical models in terms of crack pattern (at maximum displacement) and force-displacement diagrams for confined walls a) unreinforced wall with vertical joints unfilled (W2.4); b) horizontally reinforced masonry with reinforcement anchored in the masonry, and with vertical joints unfilled (W2.5); c) horizontally reinforced masonry with reinforcement anchored in the concrete tie-columns, and with vertical joints unfilled (W2.6).
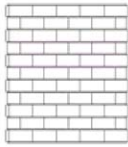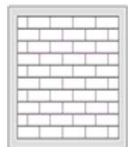
Table 1. Type and designation of specimens tested.

Typology and designation of walls			Mortar		Horizontal reinforcement	Confining elements
			Bed joint	Vertical joint		
Non-confined	Unreinforced with vertical joint unfilled	W2.1	√			
Non-confined	Unreinforced with vertical joint filled	W2.2	√	√		
Non-confined	Reinforced with vertical joint unfilled	W2.3	√		√	
Confined	Unreinforced	W2.4	√			√
Confined	Reinforced with reinforcement anchored in the masonry only	W2.5	√		√ anchored in the masonry	√
Confined	Reinforced with reinforcement anchored in the concrete tie columns	W2.6	√		√ anchored to concrete tie columns	√

Table 2. Input material parameters for the numerical model.

Material	E [N/mm²]	ν [-]	f_t [N/mm²]	G_f [N/mm]	f_c [N/mm²]	G_c [N/mm]	β [-]
Masonry	2500	0.13	0.40/0.50[a]	0.05	2.80	4.48	0.125
Concrete	31500	0.15	2.47	0.56	31.5	7.80	0.150
steel beams	200000	0.30	-	-	-	-	-

[a] value adopted for non-confined masonry wall with vertical joint filled.